Supporting Information for

Tuning the Stability of DNA Nanotubes with Salt

Supriyo Naskar[§], Mounika Gosika[§], Himanshu Joshi[§, †], Prabal K Maiti[§, *]

[§] Center for Condensed Matter Theory, Department of Physics, Indian Institute of Science, Bangalore 560012, India

[†] **Current Address:** Department of Physics, University of Illinois at Urbana-Champaign, Urbana, Illinois 61801, United States

*** Corresponding author. E-mail: maiti@iisc.ac.in,**

Tel: (091)80-2293-2865

1. Sequence and Crossover Design of the DNT

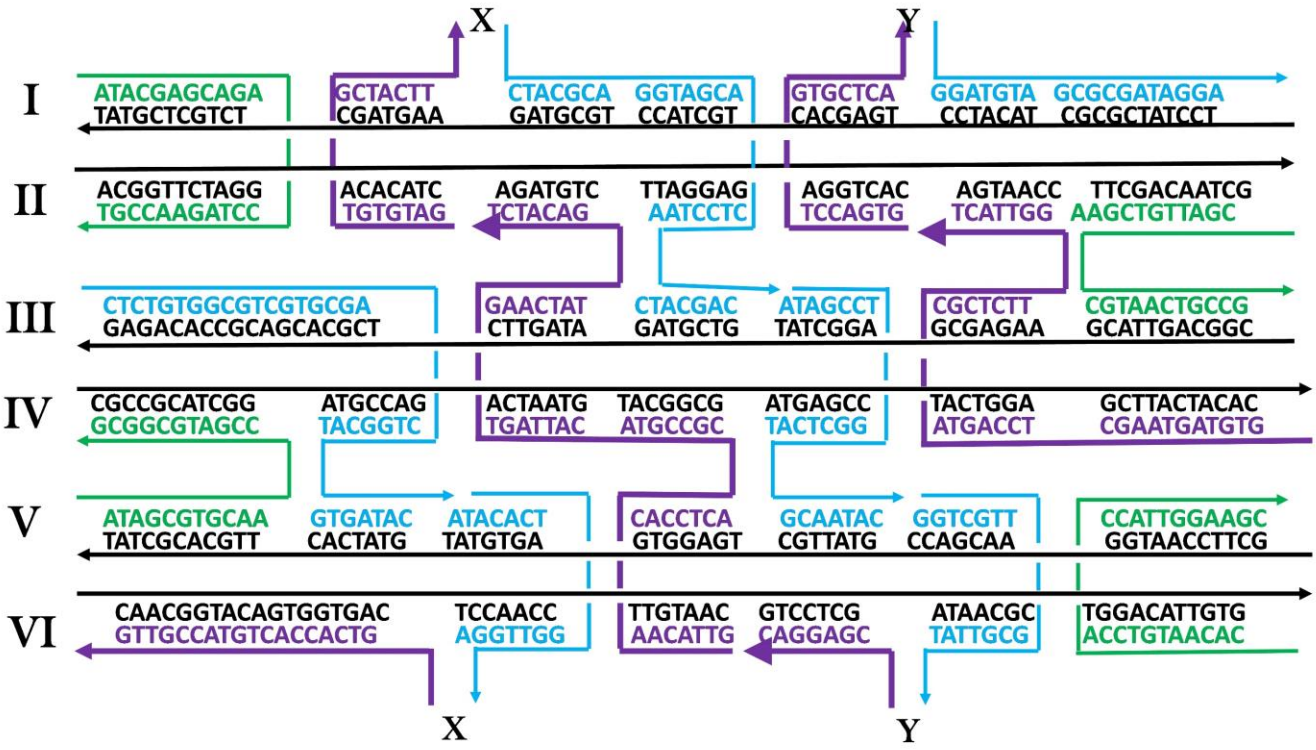

Figure S1. Schematic Diagram of the DNT crossovers with sequence. The Design is regenerated from the original experimental design by Wang et. al.[1] by removing the sticky ends on the both sides. The arrows represent the polarity of the DNA from 5' to 3'. Different Colors represents different oligonucleotide strands and by roman numbering DNA duplexes are shown. The position X and Y are the place where the cylindrical bundle closes.

Table S1: Details of the Simulated Systems

Molarity	0 M	0.5 M	1 M
Total number of atoms	215564	214764	214687
Number of Na^+	664	1446	2228
Number of Cl^-	0	782	1564
Number of Water molecules	64403	63615	63068
Rectangular Box dimension [Å]	[106 101 242]	[106 101 242]	[106 101 242]

2. Table S2: Helicoidal Parameters of the DNTs

(a) Base Pair Parameters

Snapshot Time	Ionic concentration	Shear (Å)	Stretch (Å)	Stagger (Å)	Buckle (degrees)	Propeller (degrees)	Opening (degrees)
average of the last 20 ns of the 200 ns simulation	0 M	0.00 (± 0.01)	-0.02 (±0.01)	0.05 (±0.01)	0.69 (±0.47)	-10.96 (±0.28)	0.31 (±0.27)
	0.5 M	-0.00 (± 0.01)	-0.02 (± 0.00)	0.06 (±0.01)	-0.84 (± 0.52)	-11.21 (± 0.34)	0.39 (±0.34)
	1 M	0.01 (±0.01)	-0.03 (± 0.01)	0.05 (±0.01)	0.65 (±0.45)	-11.37 (±0.29)	0.26 (±0.25)
Built		0.00 (±0.08)	-0.12 (±0.03)	0.0 (±0.0)	0.0 (±0.05)	-0.03 (±0.02)	-5.87 (±1.19)

(b) Base Step Parameters

Snapshot Time	Ionic concentration	Shift (Å)	Slide (Å)	Rise (Å)	Tilt (degrees)	Roll (degrees)	Twist (degrees)
average of the last 20 ns of the 200 ns simulation	0 M	-0.00 (± 0.02)	-0.13 (±0.02)	3.31 (±0.01)	-0.04 (±0.14)	2.25 (±0.21)	34.43 (±0.17)
	0.5 M	0.00 (± 0.02)	-0.10 (± 0.02)	3.30 (±0.01)	0.03 (± 0.17)	2.08 (± 0.27)	34.54 (±0.22)
	1 M	-0.01 (±0.01)	-0.04 (± 0.02)	3.26 (±0.01)	-0.12 (±0.14)	1.71 (±0.19)	34.38 (±0.16)
Built		0.00 (±0.03)	-0.28 (±0.03)	3.37 (±0.01)	0.01 (±0.47)	-3.09 (±0.20)	34.14 (±0.90)

(c) Helical Parameters

Snapshot Time	Ionic concentration	X-disp. (Å)	Y-disp. (Å)	Helical Rise (Å)	Inclination (degrees)	Tip (degrees)	Helical Twist (degrees)
average of the last 20 ns of the 200 ns simulation	0 M	-0.73 (± 0.05)	-0.00 (±0.02)	3.23 (±0.01)	4.28 (±0.31)	0.26 (±0.19)	35.5 (±0.24)
	0.5 M	-0.66 (± 0.05)	-0.00 (± 0.03)	3.21 (±0.01)	4.02 (± 0.353)	0.40 (± 0.21)	35.61 (±0.32)
	1 M	-0.49 (±0.04)	0.02 (± 0.04)	3.19 (±0.01)	3.42 (±0.28)	0.25 (±0.20)	35.51 (±0.22)
Built		0.02 (±0.03)	0.00 (±0.02)	3.38 (±0.01)	-5.26 (±0.38)	-0.02 (±0.8)	34.28 (±0.89)

3. Ion Distribution around DNTs

Cylindrical Distribution Function

We divide the system into small cylinders of a height equivalent to the DNT length and a radius starting from 0.5 Å to 100 Å with a bin width of 0.5 Å. Last 100 ns of the 200 ns long l MD simulation is taken for the analysis. The distribution is averaged over three sets of simulation. We then projected the distributions on to the x-y plane to comprehend the results better [See figure S2 (a), (b), (c)].

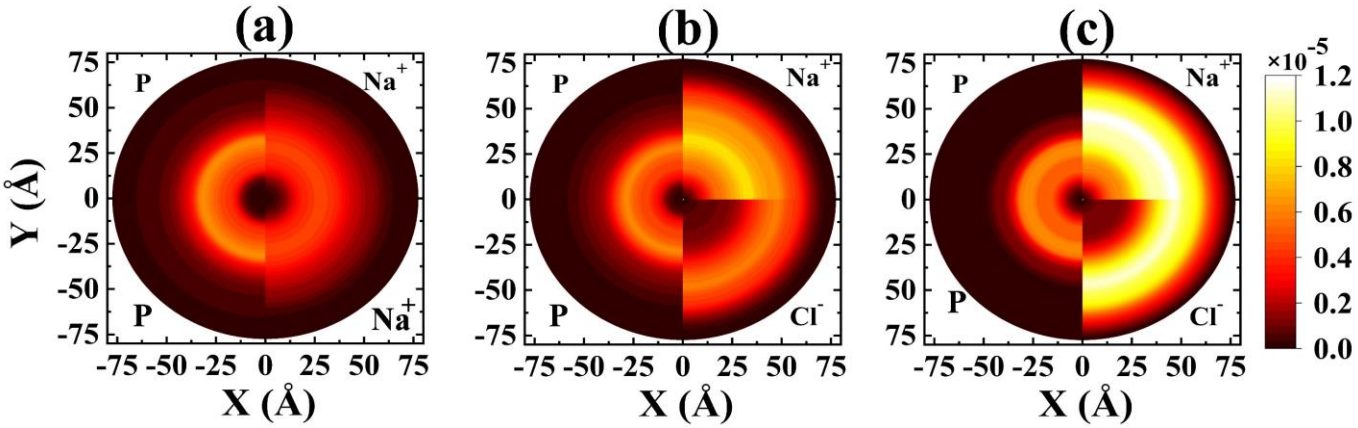

Figure S2. Cylindrical number density distribution of various ions in the system at (a) 0 M (b) 0.5 M, and (c) 1 M NaCl concentrations respectively. The colour bar is representing the scale of the number density. The length of the cylindrical grid is equivalent to that of the DNT and the bin-width used for the radii is 0.5 Å. All the plots are obtained after averaging over last 100 ns of the MD trajectory and over three independent simulation data sets.

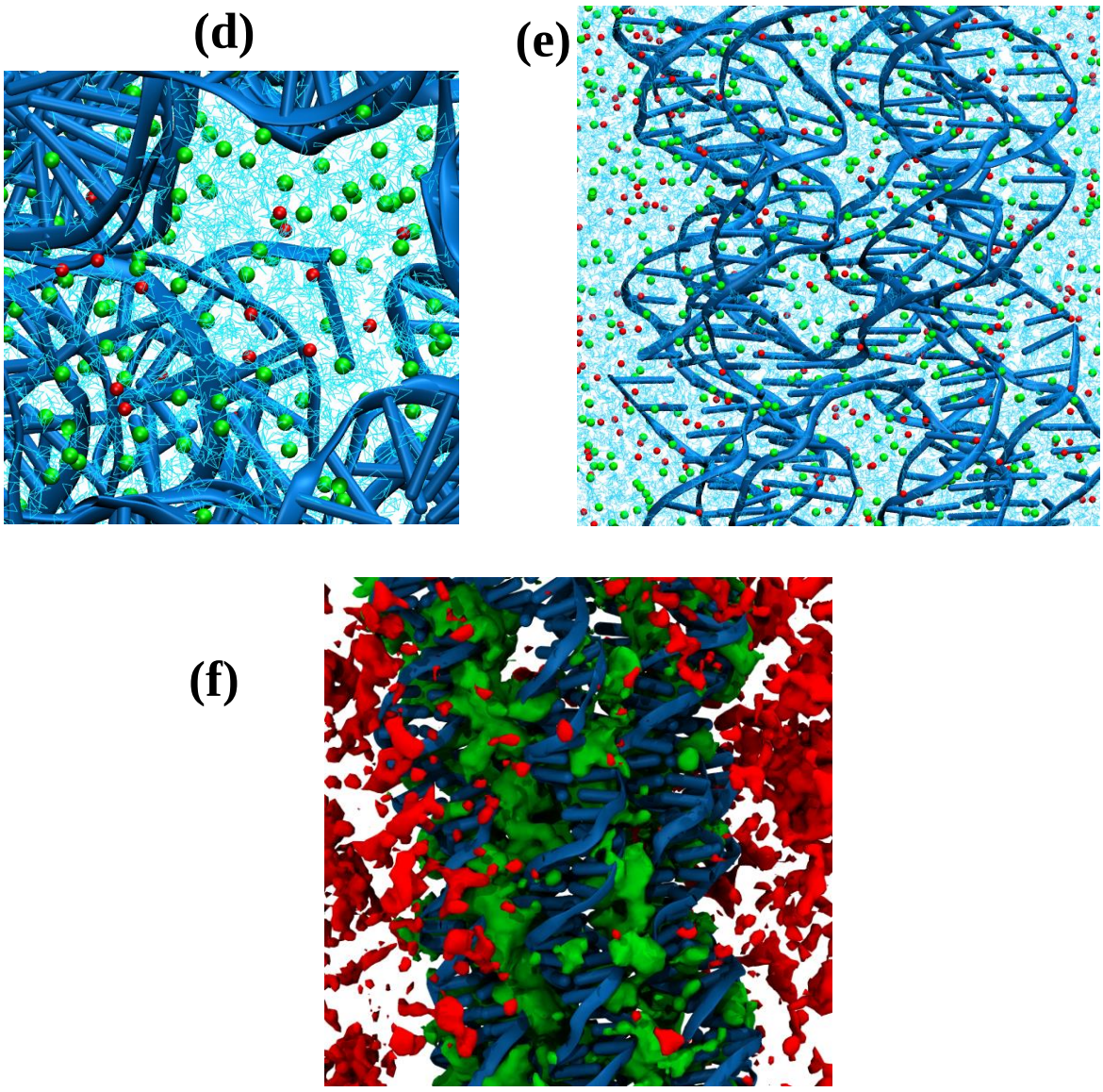

Figure S2. Porous nature of the DNT walls allows water and ions to breach into the nanopore. The green and red dots are Na^+ and Cl^- ions respectively and the cyan lines are the waters. The snapshots are taken from the (d) 0.5 M and (e) 1 M system. (f) Density map of Na^+ (green) and Cl^- (red) around the DNTs for 0.5 M system. Na^+ ions are likely to be found around negatively charged DNA backbones whereas Cl^- ions go away from the backbones because of the electrostatic repulsions. The analysis is done using VOLMAP tool of VMD.

4. Analysis of the Each Trajectories

(a) RMSD

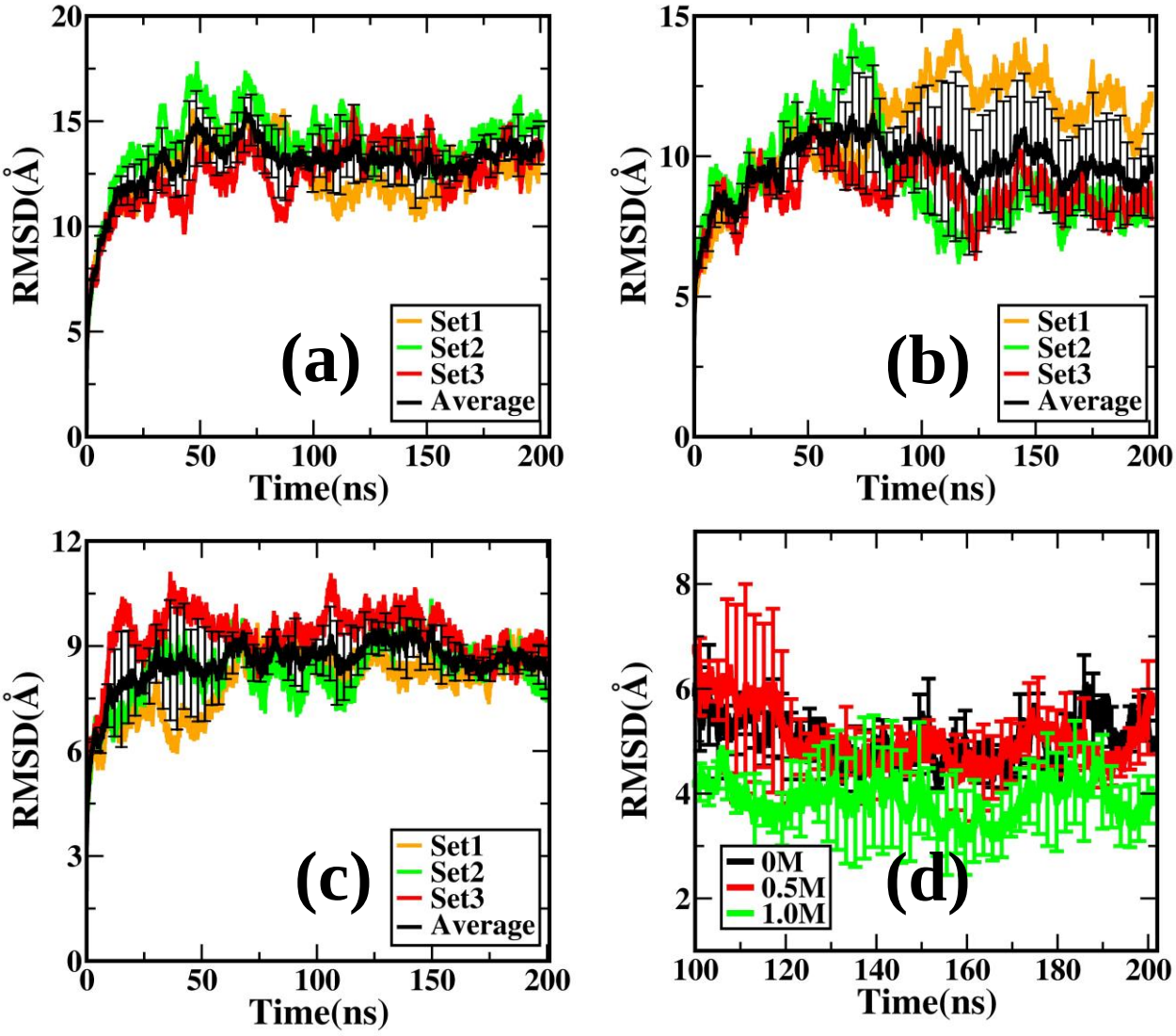

Figure S3. Root mean square deviation of the individual trajectories for NaCl concentration of (a) 0 M (b) 0.5 M and (c) 1 M concentration. RMSD is calculated for non-hydrogen atoms. (d) RMSD for each of the system with respect to the last 100 ns average structure.

(b) RMSF

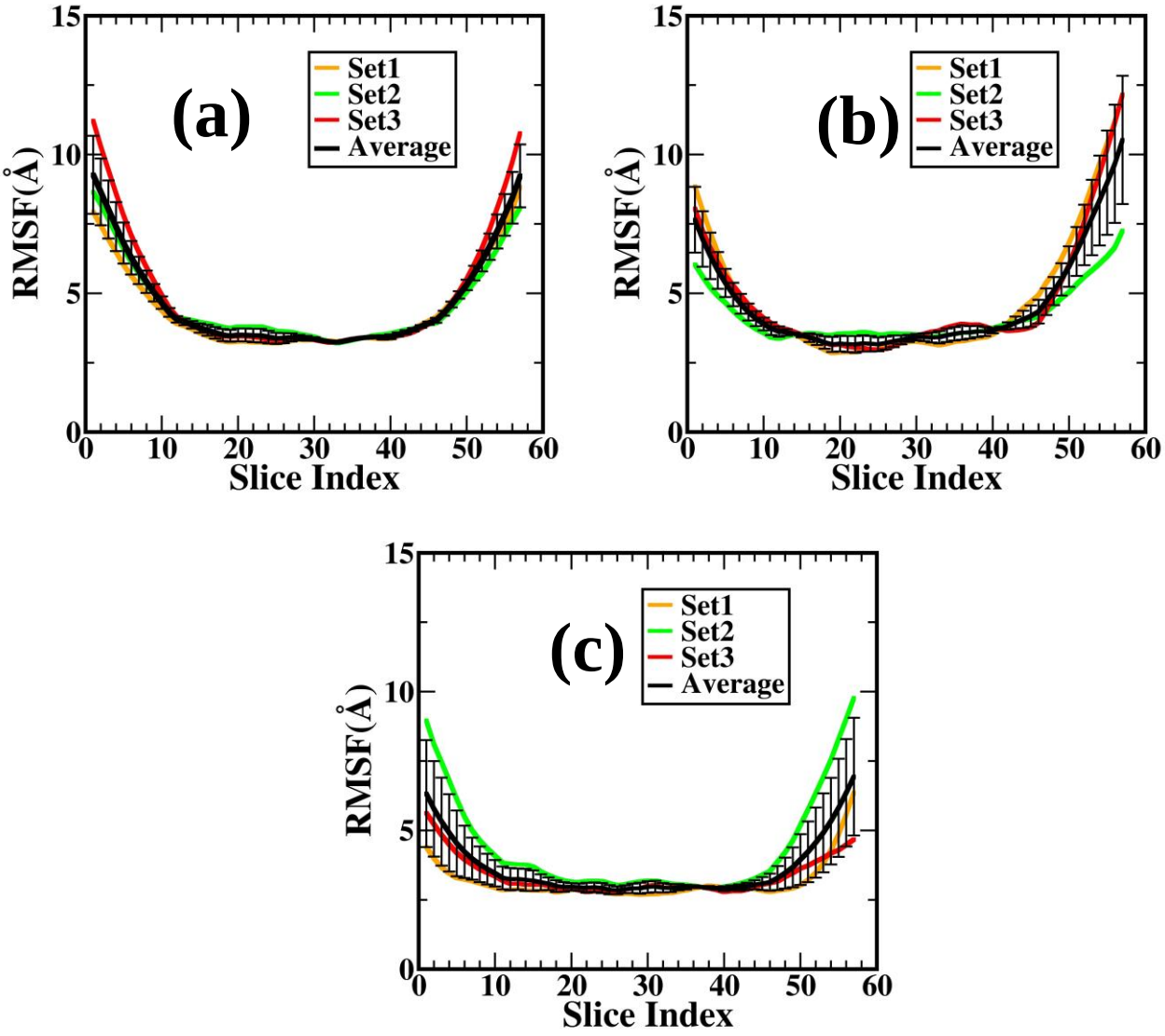

Figure S4. Root mean square fluctuation of the individual trajectories for NaCl concentration of (a) 0 M (b) 0.5 M and (c) 1 M concentration. The data is for the last 100 ns of the simulation.

(c) Radius of the Pore of the Nanotube

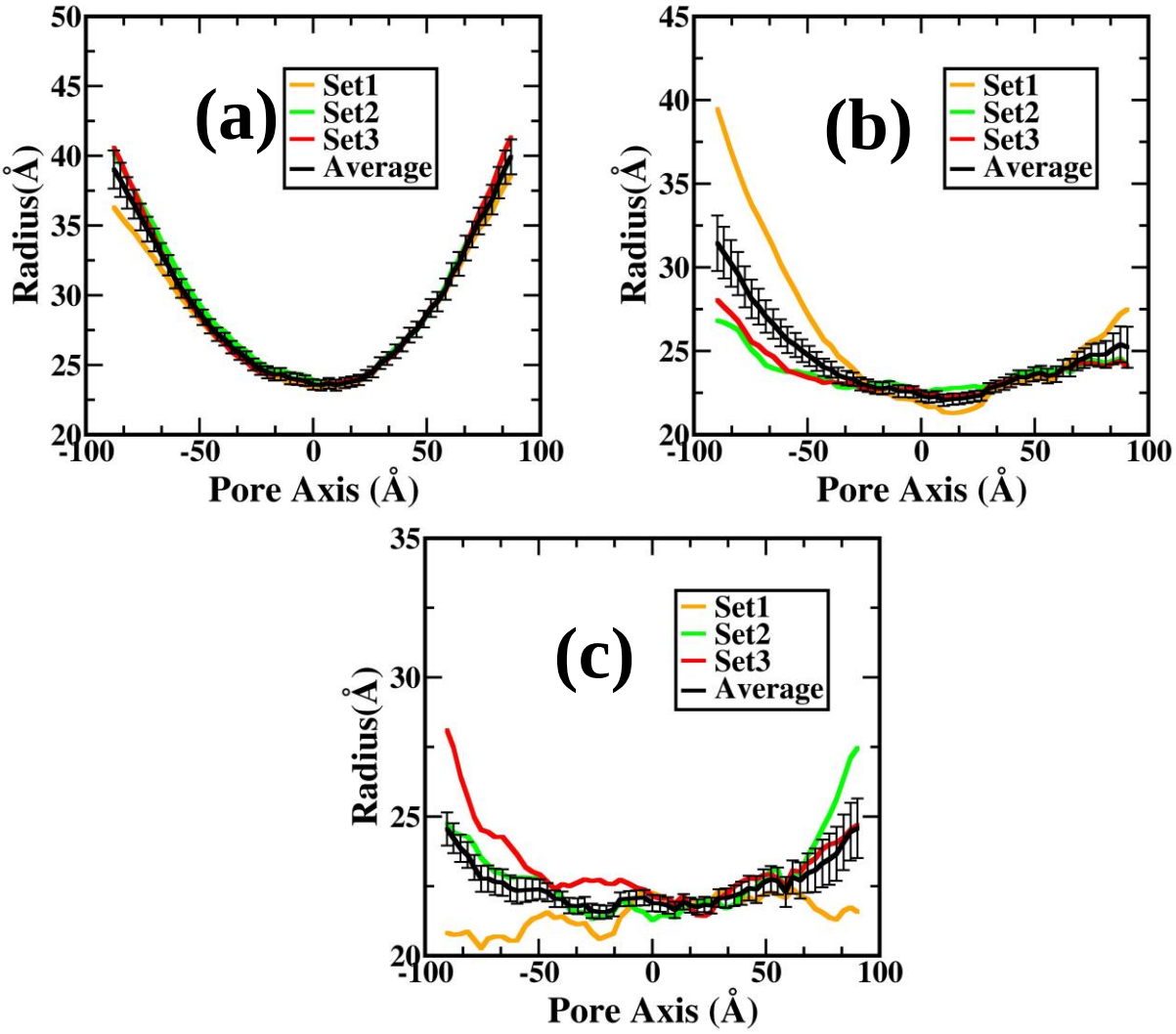

Figure S5. Radius of the pore of the DNTs of the individual trajectories for NaCl concentration of (a) 0 M (b) 0.5 M and (c) 1 M concentration. The data is time averaged for the last 100 ns of the simulation.

Table S3: Average Radius of the DNT Pore as a Function of NaCl Molarity.

Molarity	**0 M**	**0.5 M**	**1 M**
Average radius of the nanopore (Å)	29.30 ± 5.07	24.42 ± 2.29	22.52 ± 0.80

(d) Contour Length Distribution

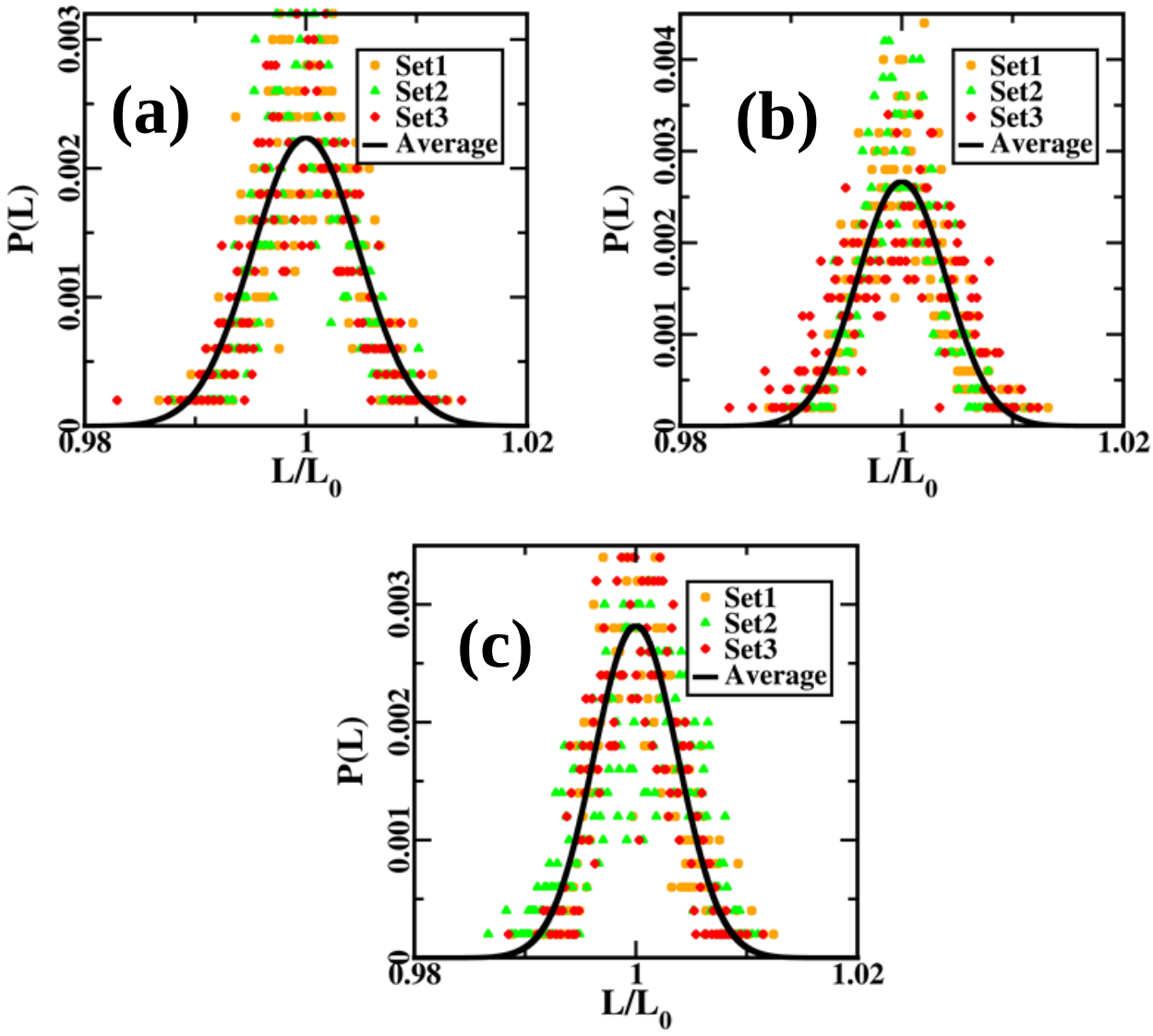

Figure S6. Contour length distribution of the DNTs of the individual trajectories for NaCl concentration of (a) 0 M (b) 0.5 M and (c) 1 M concentration. The data is time averaged for the last 100 ns of the simulation.

(e) Bending Angle Distribution

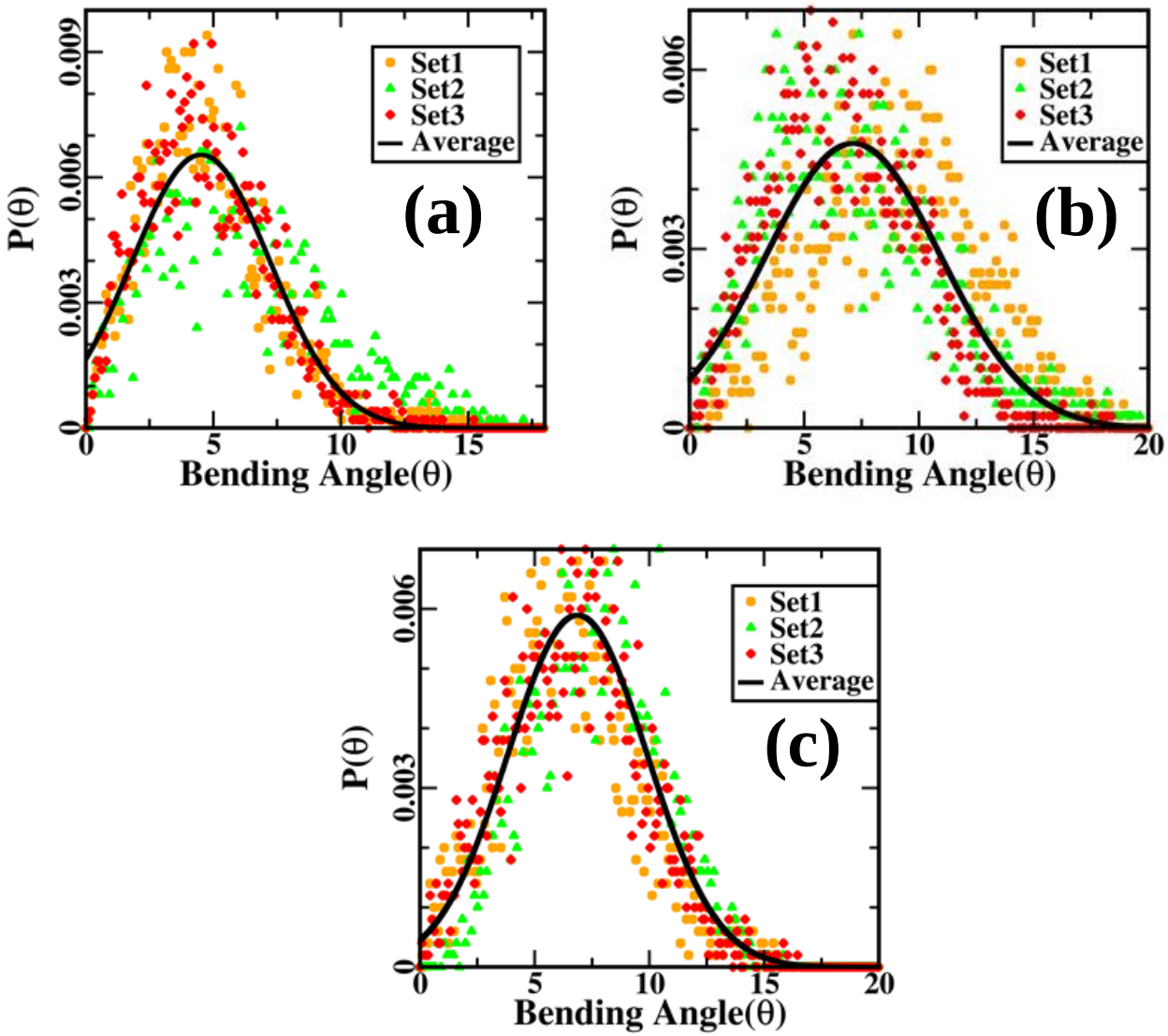

Figure S7. Bending angle distribution of the DNTs of the individual trajectories for NaCl concentration of (a) 0 M (b) 0.5 M and (c) 1 M concentration. The data is time averaged for the last 100 ns of the simulation.

5. Analysis with Three Other NaCl Salt Concentration (0.25 M, 0.75 M, 1.25 M)

We have run three simulations of the DNT systems with salt concentration 0.25 M, 0.75 M, and 1.25 M for 200 ns. The details of the systems are given below,

Table S4: Details of the simulated systems

Molarity	**0.25 M**	**0.75 M**	**1.25 M**
Total number of atoms	215564	214550	215001
Number of K+	1055	1837	2619
Number of Cl-	391	1173	1955
Number of Water molecules	63946	63283	62912
Rectangular Box dimension [Å]	[106 101 242]	[106 101 242]	[106 101 242]

(a) Final Snapshots after 200 ns for the Systems with NaCl Salt Concentration 0.25 M, 0.75 M, 1.25 M

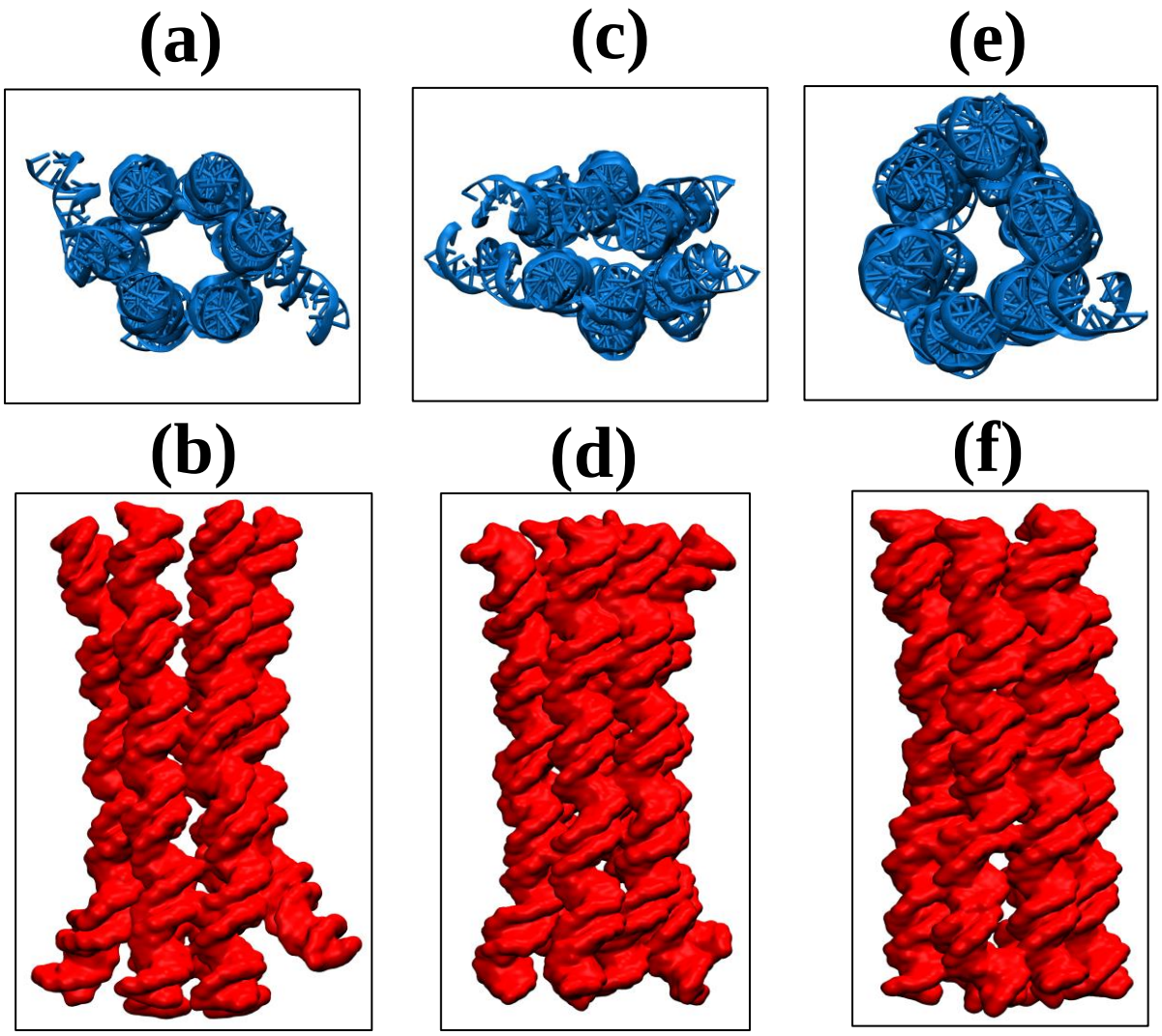

Figure S8. (a) Top view of the system with 0.25 M molarity of NaCl. (b) Same system with a side view. (c) Top view and (d) Side view of the system contains 0.75 M NaCl. (e) Top view and (f) Side view of the system contains 1.25 M NaCl.

(b) Effect of NaCl Salt Concentration on the Convergence of Structures

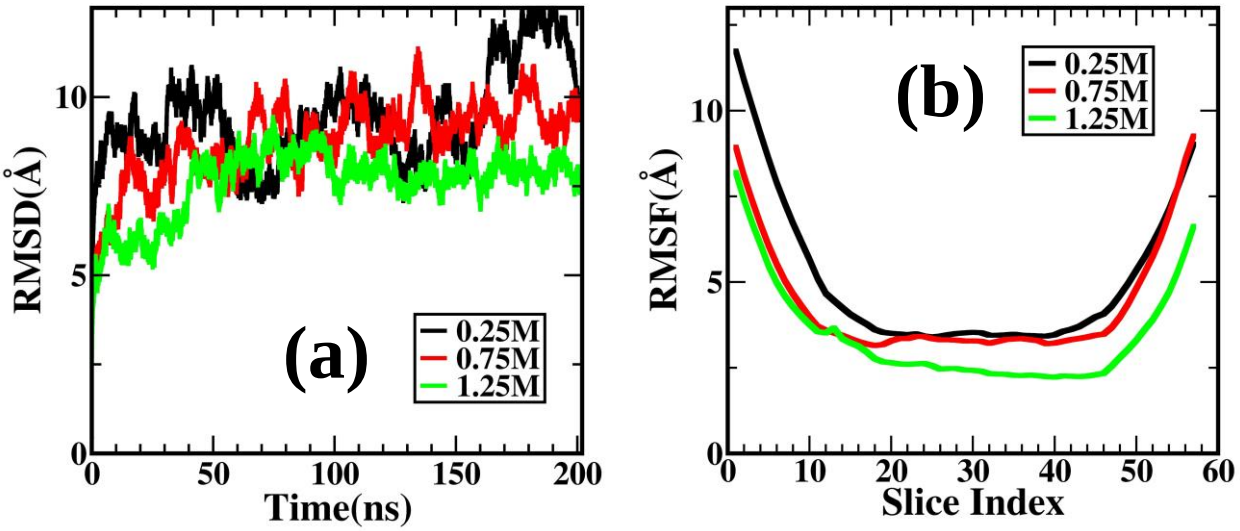

Figure S9. (a) The time evolution of the RMSD profiles of the DNTs for the three different NaCl salt concentration. RMSD is calculated with respect to the initial energy minimized structure of the DNTs. The trend in the decrement of the RMSD with increasing salt concentration is clear from the above graph. (b) Average RMSF for last 100 ns of the DNTs as function of the Slice index. Fluctuation in the terminal region is most which is decreasing with increasing salt concentration, though the central region of the DNTs are stable for all the systems.

(c) Time Evolution of the Pore Radius for the systems with KCl salt

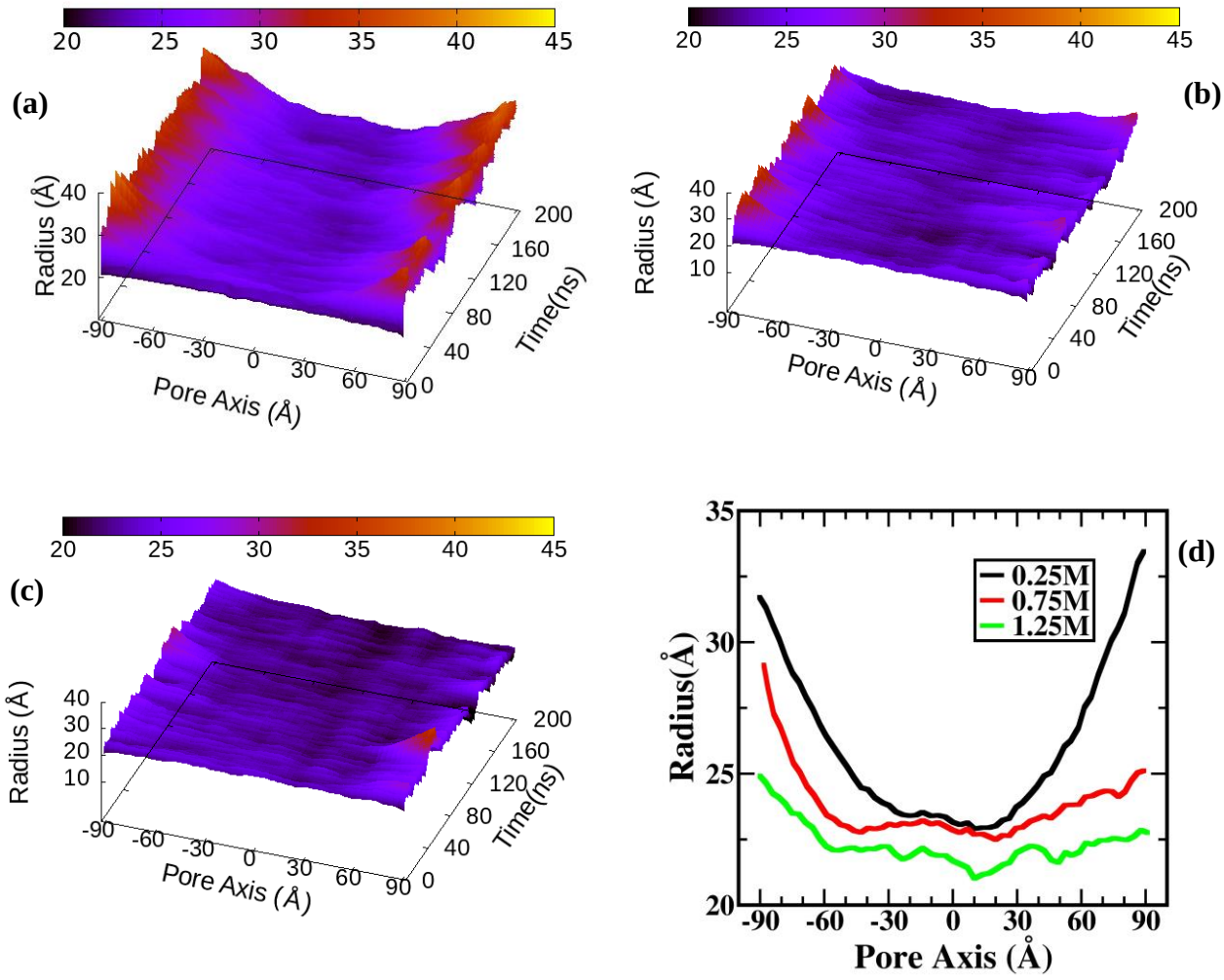

Figure S10. Time Evolution of the average radius profile along the pore axis of the DNTs for the system with NaCl molarity (a) 0.25 M (b) 0.75 M, and (c)1.25 M respectively. (d) Final radius profile of the DNTs averaged over the last 100 ns.

(d) Stretch Modulus from Contour Length Distribution

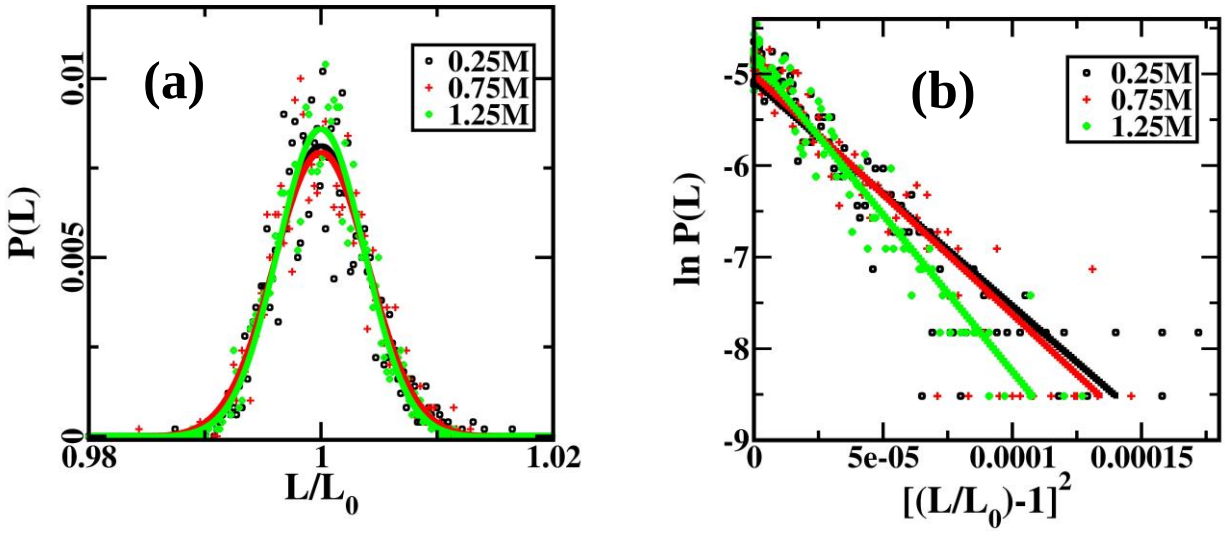

Molarity	0 M	0.25 M	0.5 M	0.75 M	1 M	1.25 M
Stretch Modulus with NaCl (pN)	8294.87 ± 148.19	9936.18 ± 269.29	10540.9 ± 148.13	10777.45 ± 268.35	13066.8 ± 155.91	14071.83 ± 261.35

Figure S11. (a) Probability distribution of the normalized contour length of the DNTs. The data is averaged over the las 100 ns of the whole simulation. (b) Logarithm of the probability as a function of $\left(\frac{L}{L_0}-1\right)^2$. From the slope of the graphs, stretch modulus has been extracted. In the table calculated stretch modulus for NaCl systems have been listed.

(e) Persistence Length from Bending Length Distribution and Microscopic Elastic theory (MET)

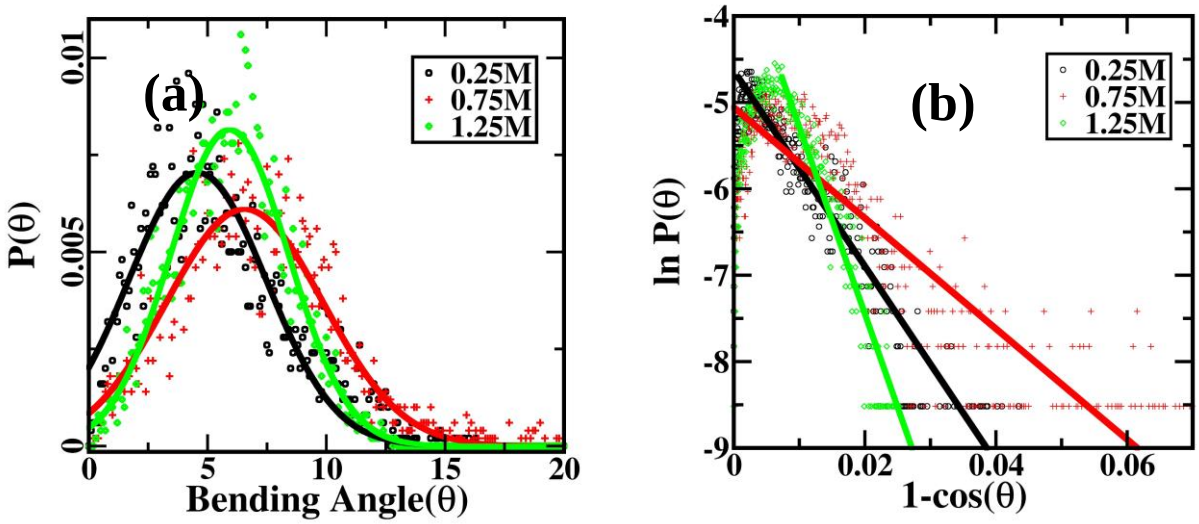

Molarity	0 M	0.25 M	0.5 M	0.75 M	1 M	1.25 M
Persistence Length from Microscopic Elastic theory (μm)	6.36 ± 0.11	7.72 ± 0.21	8.27 ± 0.12	8.49 ± 0.21	10.40 ± 0.12	11.21 ± 0.21
Persistence Length from Bending Angle Distribution (μm)	2.45 ± 0.04	2.32 ± 0.06	1.86 ± 0.02	1.29 ± 0.05	3.01 ± 0.04	4.35 ± 0.11

Figure S12. (a) Probability distribution of the bending angle for the last 80 ns trajectory. (b) Log of the $P(\theta)$ versus $1 - cos\theta$. Persistence length has been calculated from the slope of the graph. In the table calculated persistence length using two different methods for NaCl systems have been listed.

6. Analysis with KCl Salt

We have run three simulations of the DNT systems with KCl salt concentration 0 M, 0.5 M, and 1 M for 100 ns. The details of the systems are given below,

Table S5: Details of the simulated systems

Molarity	**0 M**	**0.5 M**	**1 M**
Total number of atoms	215564	215625	216505
Number of K+	664	1446	2228
Number of Cl-	0	782	1564
Number of Water molecules	64403	63902	63674
Rectangular Box dimension [Å]	[106 101 242]	[106 101 242]	[106 101 242]

(f) Final Snapshots after 100 ns for the Systems with KCl Salt

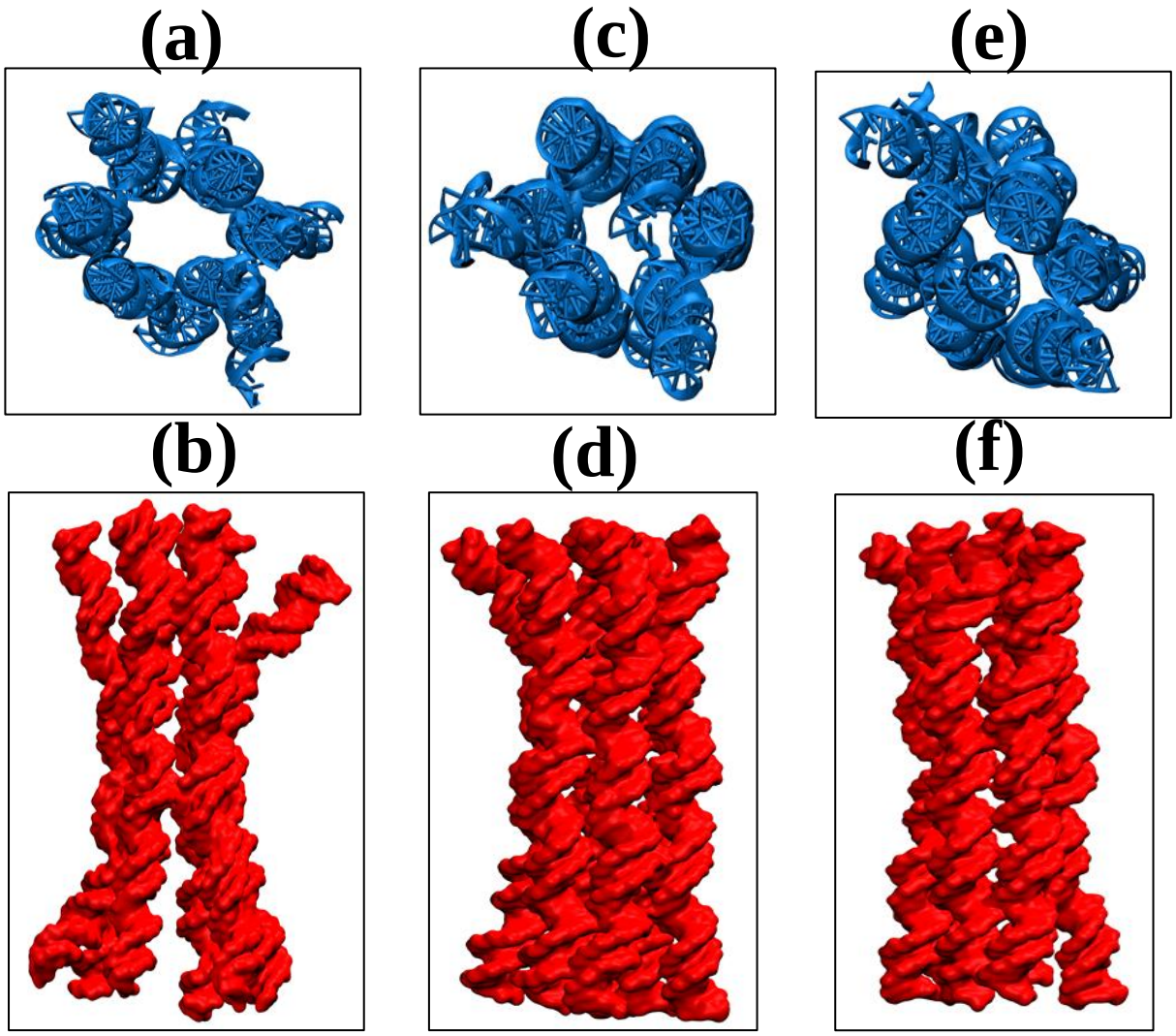

Figure S13. (a) Top view of the system with zero molarity of KCl. (b) Same system with a side view. The both terminal regions open whereas the central portion remains intact. (c) Top view and (d) Side view of the system contains 0.5 M KCl. The fluctuation in the terminal region reduces significantly in the system. (e) Top view and (f) Side view of the system contains 1 M KCl.

(g) Effect of KCl Salt Concentration on the Convergence of Structures

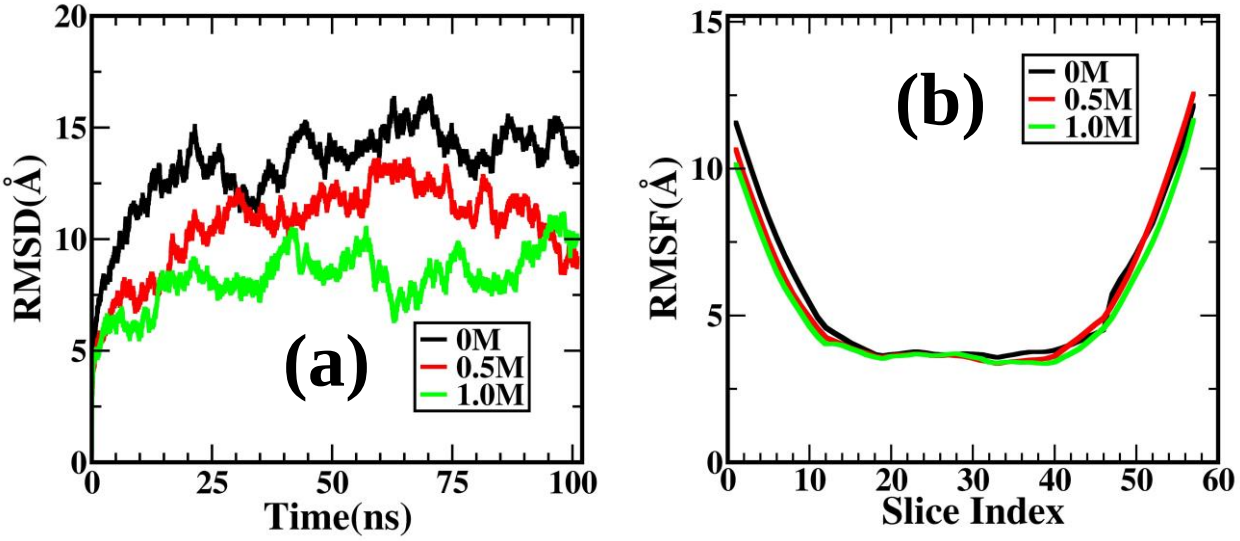

Figure S14. (a) The time evolution of the RMSD profiles of the DNTs for the three different systems. RMSD is calculated with respect to the initial energy minimized structure of the DNTs. The trend in the decrement of the RMSD with increasing salt concentration is clear from the above graph. (b) Average RMSF of the DNTs as function of the Slice index. Fluctuation in the terminal region is most which is decreasing with increasing salt concentration, though the central region of the DNTs are stable for all the systems.

(h) Time Evolution of the Pore Radius for the systems with KCl salt

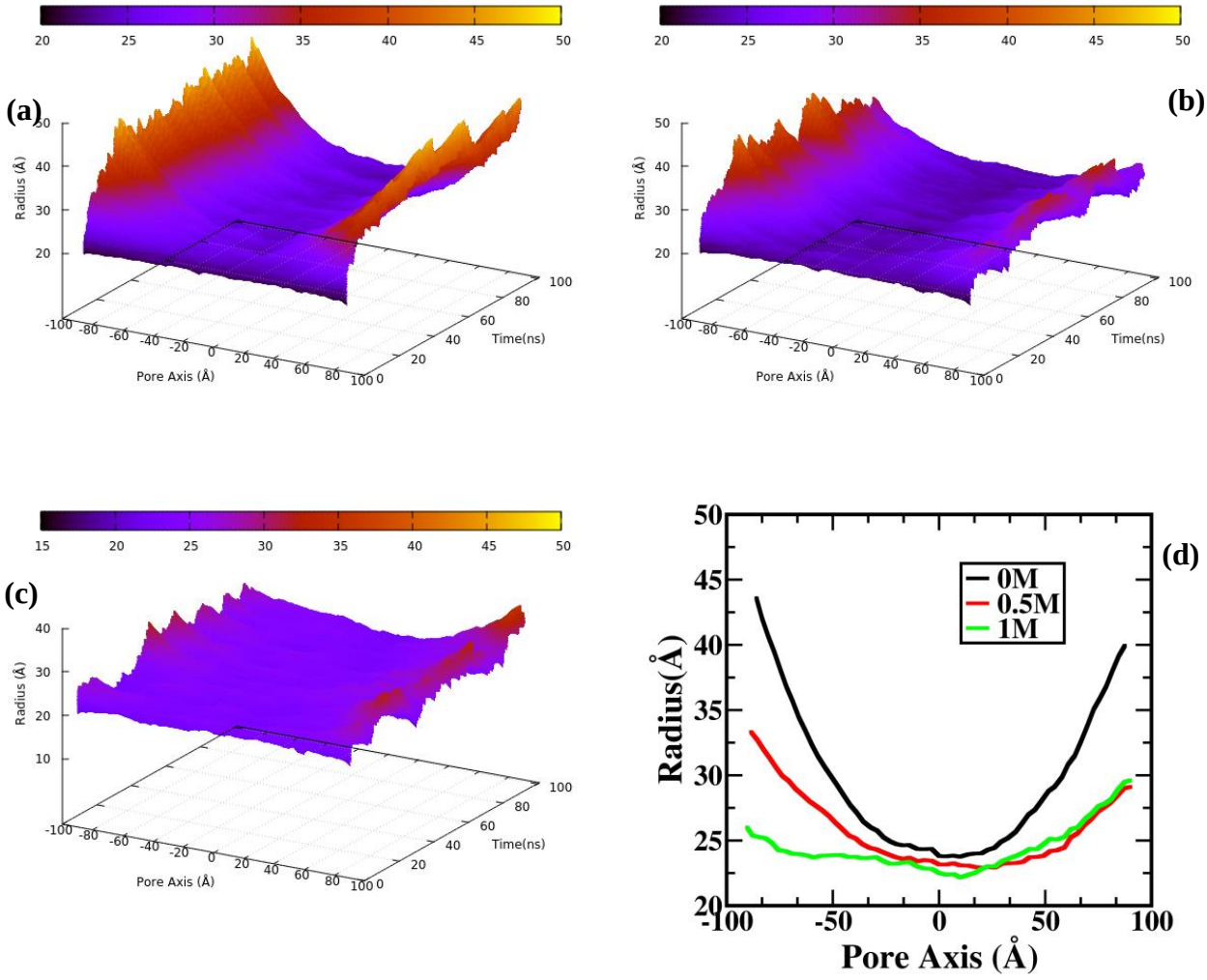

Figure S15. Time Evolution of the average radius profile along the pore axis of the DNTs for the system with KCl molarity (a) 0 M (b) 0.5 M, and (c)1 M respectively. (d) Final radius profile of the DNTs averaged over the last 80 ns.

(i) Stretch Modulus from Contour Length Distribution

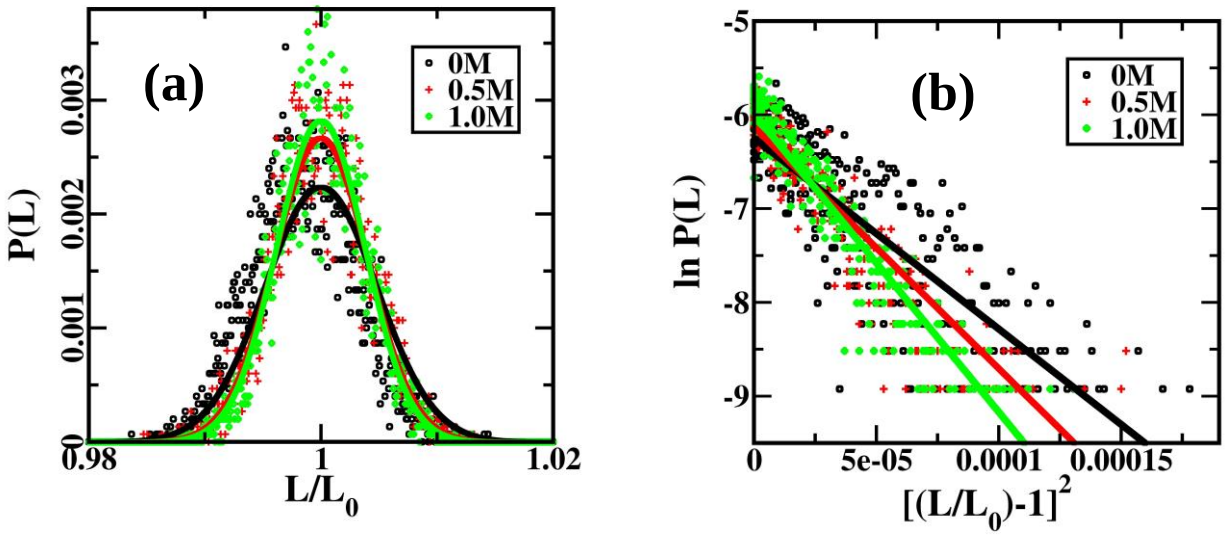

Molarity	0 M	0.5 M	1 M
Stretch Modulus with NaCl (pN)	8294.87 ± 148.19	10540.9 ± 148.13	13066.8 ± 155.91
Stretch Modulus with KCl(pN)	7811.62 ± 220.80	11860.78 ± 293.01	13167.34 ± 324.91

Figure S16. (a) Probability distribution of the normalized contour length of the DNTs. The data is averaged over the las 80 ns of the whole simulation. (b) Logarithm of the probability as a function of $\left(\frac{L}{L_0} - 1\right)^2$. From the slope of the graphs, stretch modulus has been extracted. In the table calculated stretch modulus for NaCl and KCl systems have been listed.

(j) Persistence Length from Bending Length Distribution and MET

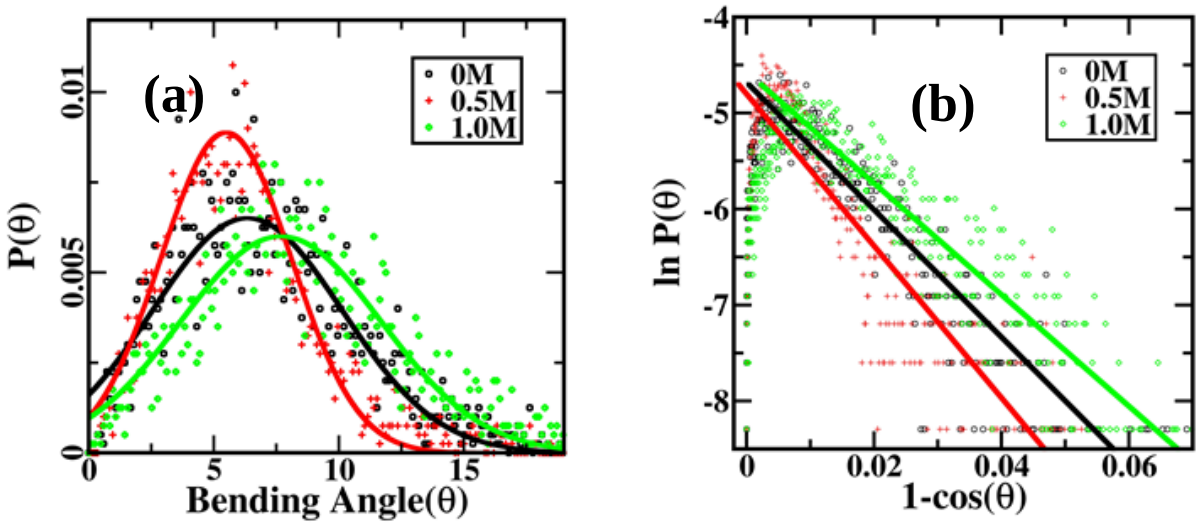

Molarity	0 M	0.5 M	1 M
Persistence Length [Using MET for NaCl system] (μm)	6.35 ± 0.11	8.28 ± 0.12	10.42 ± 0.12
Persistence Length [Using MET for KCl system] (μm)	5.98 ± 0.17	9.24 ± 0.23	10.33 ± 0.25
Persistence Length [Using bending angle distribution for NaCl system] (μm)	2.45 ± 0.04	1.86 ± 0.02	3.01 ± 0.04
Persistence Length [Using bending angle distribution for KCl system] (μm)	1.42 ± 0.04	1.59 ± 0.06	1.17 ± 0.03

Figure S17. (a) Probability distribution of the bending angle for the last 80 ns trajectory. (b) Log of the $P(\theta)$ versus $1 - cos\theta$. Persistence length has been calculated from the slope of the graph. In the table calculated persistence length for NaCl and KCl systems have been listed.

7. Analysis with $MgCl_2$ Salt

We have run Four simulations of the DNT systems with $MgCl_2$ salt concentration 0 M, 0.25 M, 0.5 M, and 1 M for 200 ns. The details of the systems are given below,

Table S6: Details of the Simulated Systems

Molarity	**0 M**	**0.25 M**	**0.5 M**	**1 M**
Total number of atoms	216288	216084	216288	216384
Number of Mg^{2+}	332	723	1114	1896
Number of Cl-	0	782	1564	3128
Number of Water molecules	64735	64296	63953	63223
Rectangular Box dimension [Å]	[106 101 242]	[106 101 242]	[106 101 242]	[106 101 242]

(a) Final Snapshots after 200 ns for the Systems with $MgCl_2$ Salt

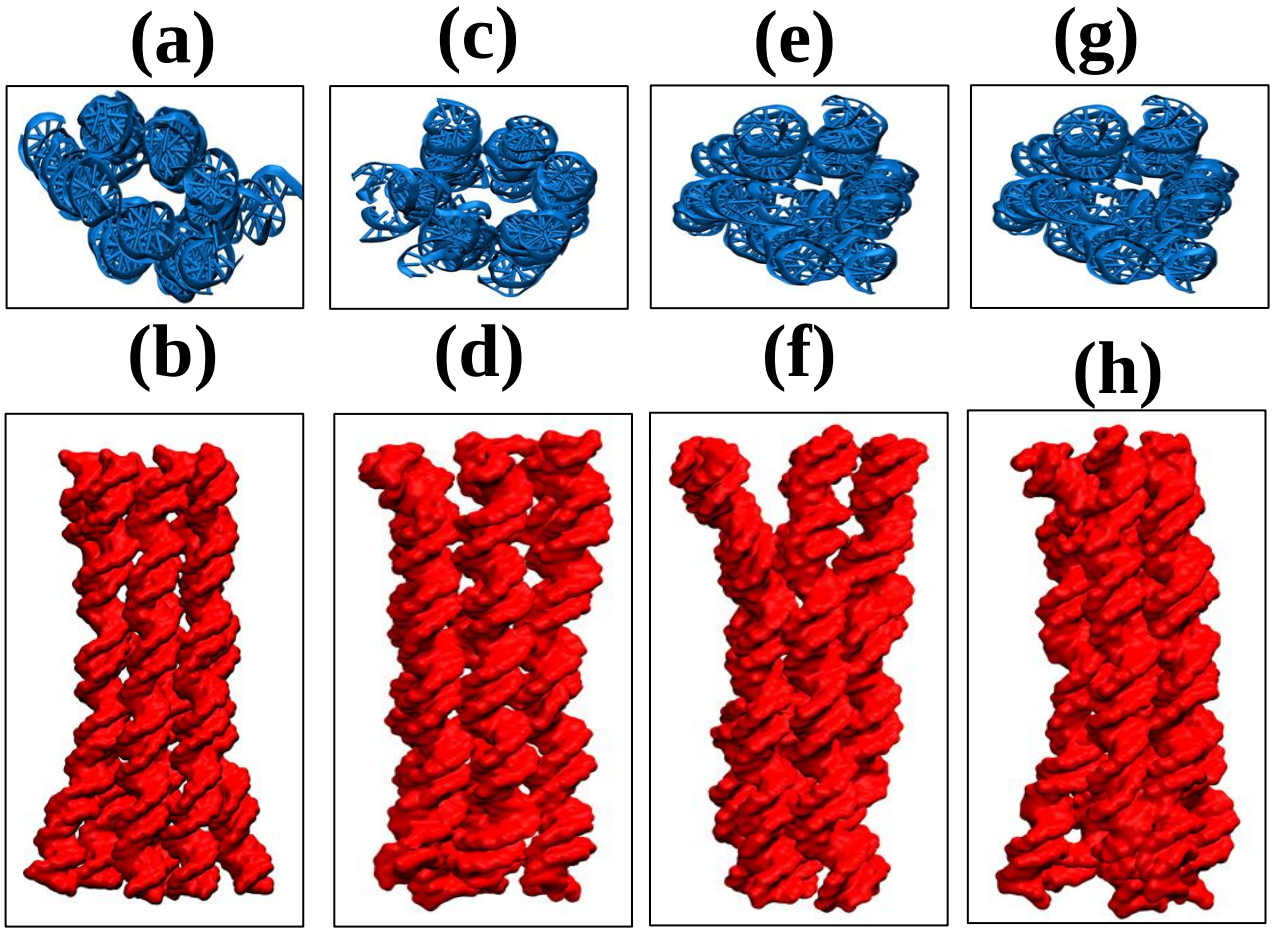

Figure S18. Instantaneous snapshots of the systems after 200 ns. (a) Top view of the system with zero molarity of $MgCl_2$. (b) Same system with a side view. The both terminal regions open whereas the central portion remains intact. (c) Top view and (d) Side view of the system contains 0.25 M $MgCl_2$. (e) Top view and (f) Side view of the system contains 0.5 M $MgCl_2$. (g) Top view and (h) Side view of the system contains 1 M $MgCl_2$. All the structures are almost equally stable. No trend of higher stability with higher salt concentration has been found for $MgCl_2$.

(b) Effect of $MgCl_2$ Salt Concentration on the Convergence of Structures

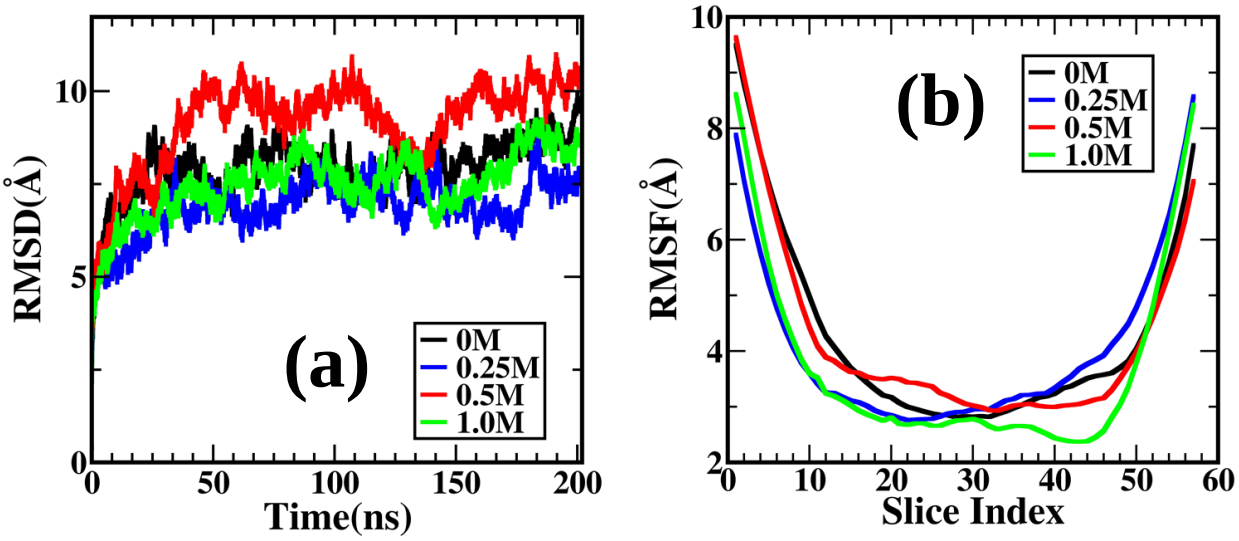

Figure S19. (a) The time evolution of the RMSD profiles of the DNTs for the Four different systems. RMSD is calculated with respect to the initial energy minimized structure of the DNTs. The trend in the decrement of the RMSD with increasing salt concentration is not found from the above graph. (b) Average RMSF of the DNTs as function of the Slice index. Fluctuation in the terminal region is high and the central region of the DNTs are stable for all the systems.

(c) Time Evolution of the Pore Radius for the Systems with $MgCl_2$ salt

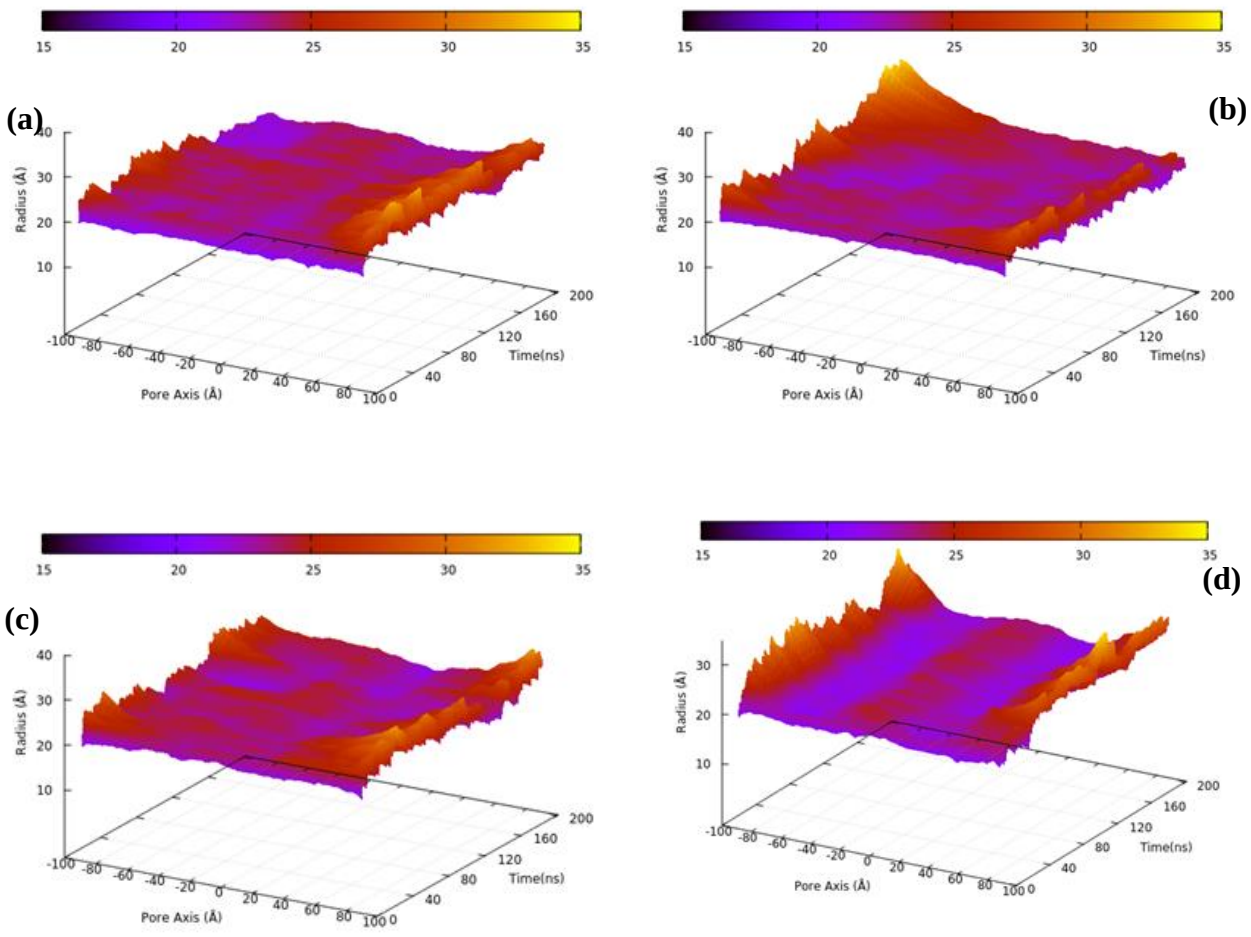

Figure S20. Time Evolution of the average radius profile along the pore axis of the DNTs for the system with $MgCl_2$ molarity (a) 0 M (b) 0.25 M, (c) 0.5 M, and (d) 1 M respectively.

(d) Stretch Modulus from Contour Length Distribution

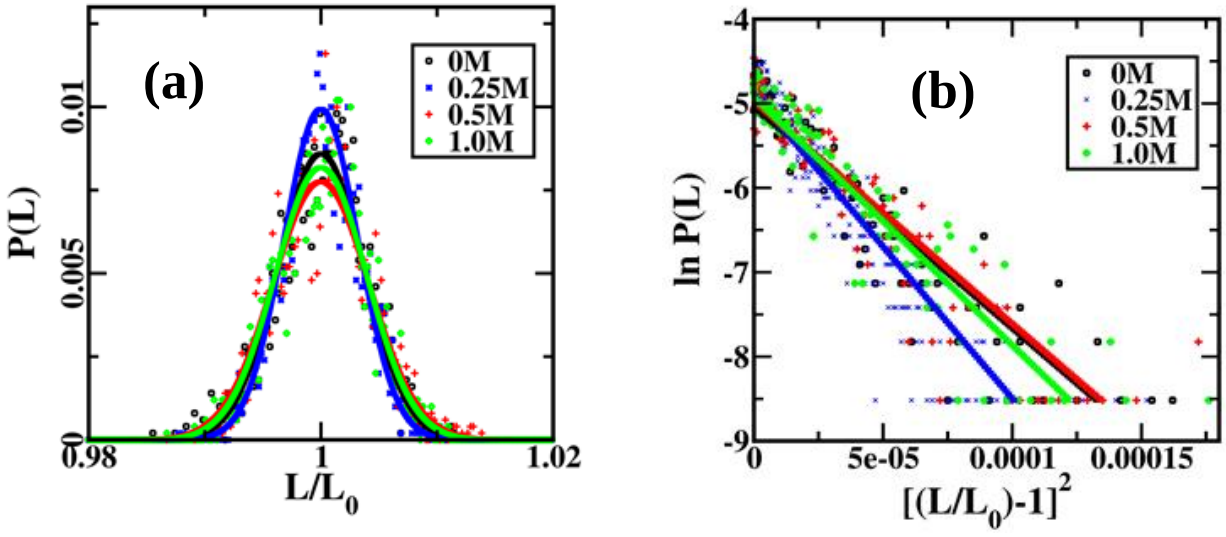

Molarity	0 M	0.25 M	0.5 M	1 M
Stretch Modulus with NaCl (pN)	8294.87 ± 148.19	9936.18 ± 269.29	10540.9 ± 148.13	13066.8 ± 155.91
Stretch Modulus with $MgCl_2$(pN)	10755.88 ± 299.29	14750.91 ± 400.40	10742.90 ± 241.05	11986.36 ± 263.53

Figure S21. (a) Probability distribution of the normalized contour length of the DNTs. The data is averaged over the las 80 ns of the whole simulation. (b) Logarithm of the probability as a function of $\left(\frac{L}{L_0}-1\right)^2$. From the slope of the graphs, stretch modulus has been extracted. In the table calculated stretch modulus for NaCl and $MgCl_2$ systems have been listed.

(e) Persistence Length from Bending Length Distribution and MET

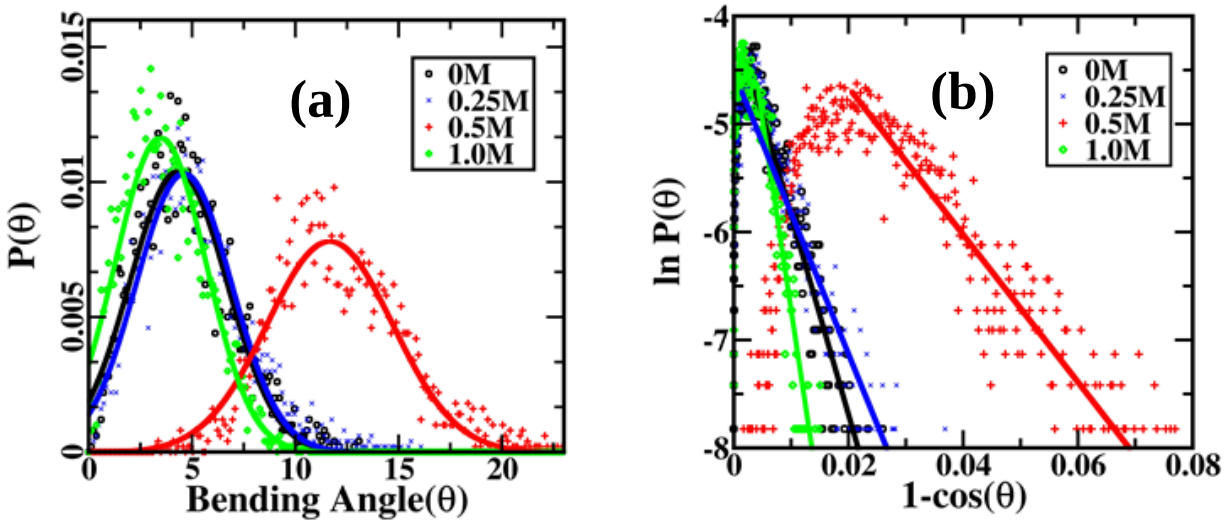

Molarity	0 M	0.25 M	0.5 M	1 M
Persistence Length [Using MET for NaCl system] (μm)	6.36 ± 0.11	7.72 ± 0.21	8.27 ± 0.12	10.40 ± 0.12
Persistence Length [Using MET for $MgCl_2$ system] (μm)	8.55 ± 0.24	11.56 ± 0.31	8.46 ± 0.19	9.46 ± 0.20
Persistence Length [Using bending angle distribution for NaCl system] (μm)	2.45 ± 0.04	2.32 ± 0.06	1.86 ± 0.02	3.01 ± 0.04
Persistence Length [Using bending angle distribution for $MgCl_2$ system] (μm)	3.72 ± 0.16	2.63 ± 0.10	1.27 ± 0.03	7.17 ± 0.36

Figure S22. (a) Probability distribution of the bending angle for the last 100 ns trajectory. (b) Log of the $P(\theta)$ versus $1 - cos\theta$. Persistence length has been calculated from the slope of the graph. In the table calculated persistence length for NaCl and $MgCl_2$ systems have been listed.

From these analyses, we can say all the DNT structures are almost equally stable irrespective of the $MgCl_2$ concentration. Our results are also in agreement with experimental findings[2].

Reference

1. Wang, T., et al., *Design and characterization of 1D nanotubes and 2D periodic arrays self-assembled from DNA multi-helix bundles*. Journal of the American Chemical Society, 2012. **134**(3): p. 1606-1616.
2. Kielar, C., et al., *On the Stability of DNA Origami Nanostructures in Low-Magnesium Buffers*. Angewandte Chemie, 2018.